Supporting Material for "How capping protein enhances actin filament growth and nucleation on biomimetic beads"

by Ruizhe Wang and A. E. Carlsson

October 1, 2015

A: Calculation of local depletion effect

We assume a quasi-static approximation to calculate the protein concentrations, in the sense that for a given number of free filaments N_f on the surface of the bead, the concentrations are assumed to have the corresponding steady-state distributions. Our approach is similar to that used by Refs. [1], [2] and [3]. The monomer concentration $[G]$ satisfies the following equation:

$$\nabla^2[G] = 0$$

The general solution is $[G] = C_1 + C_2/r$, where C_1 and C_2 are constants and r is the distance from the origin. It must satisfy the following boundary conditions:

i) The concentration matches the bulk concentration at infinity: $[G]|_{r\to\infty} = [G_0]$
ii) The number of monomers depleted by polymerization at free filament ends should equal the net influx (polymerization minus depolymerization) into the bead surface: $N_f k_{on}([G] - G_c)|_{r=r_0} = 4\pi r_0^2 D \frac{\partial [G]}{\partial r}|_{r=r_0}$, where we use the fact that the depolymerization rate of a filament is $k_{on}G_c$.

By imposing these boundary conditions on the general solution for $[G]$, we determine the constants C_1 and C_2 and obtain (for a general value of r)

$$[G] = [G_0]\left(1 - \frac{r_0}{r}\frac{N_f k_{on}}{4\pi r_0 D_m + N_f k_{on}}\right) + G_c\left(\frac{r_0}{r}\frac{N_f k_{on}}{4\pi r_0 D_m + N_f k_{on}}\right)$$

Choosing $r = r_0$ gives Eq.(4). Similarly, we obtain Eq.(5) and (6).

A parallel analysis can be used to obtain $[G]$ in terms of $[G_0]$ and the net monomer current I flowing to the bead. Then boundary condition ii) becomes $4\pi r_0^2 D \frac{\partial [G]}{\partial r}|_{r=r_0} = I$. One readily shows that the corresponding solution for $[G]$ at a general value of r is

$$[G] = [G_0]\left(1 - \frac{I}{4\pi [G_0] D_m r}\right);$$

at $r = r_0$ this gives

$$[G] = [G_0]\left(1 - \frac{I}{4\pi[G_0]D_m r_0}\right).$$

Note that this expression becomes negative when I exceeds the physical limit imposed by diffusion to a perfectly absorbing sphere.

B: Validity of model assumptions

The key assumptions and approximations not discussed in the main text are the following:

1) The local concentrations ($[G]$, $[CP]$, and $[Arp]$) change instantaneously to a quasi-steady state in response to changes in N_f. The validity of this approximation is determined by the characteristic time τ_c for the concentration field to reach steady state. At the coarsest level, the depletion hole in the protein concentration is a region of size comparable to the bead radius r_0. Accordingly, we estimate, for actin, that $\tau_c \sim \langle r_0^2 \rangle / 6D_m \sim 0.02s$, which is negligible in comparison to the time scale of tens of seconds [4] over which the number of filaments changes significantly. The times for CP and Arp2/3 complex are similarly small. The finer-scale structure of the depletion hole contains smaller spatial wavelengths, and therefore should relax even more rapidly. Therefore it is legitimate to assume that the concentration field is in quasi-steady state.

2) The diffusion coefficients in the network are assumed to be have their bulk solution values. Above we showed that actin monomers reach the bead at nearly the diffusion limit defined by the bulk diffusion coefficient. This suggests that the slowing by the actin network is fairly small, which is reasonable in view of the low packing fractions of actin networks. However, measurements on beads in cell extracts [5] showed a gel diffusion coefficient that is only 10% of the bulk solution value. We thus estimate the potential effects of such a reduction. We define $I_1 = 4\pi D_m [G'_0] r_0 = 2.2 \times 10^6 s^{-1}$ as the diffusion-limited current to the bead with no reduction in diffusion coefficient, where $D_m = 70\mu^2 s^{-1}$ [6]; $[G'_0] = 1.4\mu M$ is taken from the late-time points in Fig. S6B of Ref. [4] and $r_0 = 3\mu m$ is the value used in Ref. [4]. We have performed a steady-state diffusion profile calculation using the same formulation as in the Supplementary Material, but including a $2\mu m$ thick actin shell whose diffusion coefficient is reduced to $0.1D_m$. We find that the current to the bead surface, I_2, is only about $0.2I_1 = 4 \times 10^5 s^{-1}$. This number is much lower than the monomer flux of about $2.2 \times 10^6 s^{-1}$ that we obtained above from Fig. 5c of Ref. [4]. Thus the reduction in the diffusion coefficient cannot be as large as in Ref. [5].

Even though we do not treat slowing of diffusion by the gel, diffusion is a strong constraint in our model. The monomer addition to the bead cannot exceed the diffusion-limited upper bound $4\pi D_m r_0 [G_0]$ [7], and when the flux is close to this

value a pronounced monomer depletion region builds up around the bead.

3) The addition of actin subunits to the network during nucleation events is neglected, since the contribution of polymerization to F should be much greater than that of nucleation. This is legitimate as long as the average length $\bar{l}$ of filaments is much greater than the critical nucleus size of actin filaments. In the experiments, the number of subunits in the actin networks is about 1.5×10^8 (Fig. 5c of Ref. [4]), and the number of filaments is up to 3×10^6 (Fig. 5d of Ref. [4], after subtracting a contribution from nonspecific association given in their Fig S5), so $\bar{l} \geq 1.5 \times 10^8/(3 \times 10^6) \sim 50$ subunits. By comparison, Sept and McCammon [8] suggested that the critical nucleus is a trimer, much smaller than a typical filament. Zalevsky *et al* [9] argued that the critical nucleus for Arp2/3-based branching nucleation is smaller than a trimer. We have performed additional calculations with this effect included, and the values of F and N changed by less than 2%.

4) Capped filaments do not nucleate new branches. This assumption is expected to hold reasonably well, since retrograde flow will cause a capped filament to rapidly leave the ActA-coated bead surface and lose its branching ability. This occurs in the stochastic simulations described below. Allowing capped filaments to nucleate new branches would strengthen the effect found below, where CP enhances filament nucleation.

5) The local protein concentrations at the bead surface are determined by the number of filaments according to the mean field theory of Eqs. (5-7) of the main text. Ref. [10] studied the diffusion-limited ligand binding rate to randomly placed receptors on a sphere, comparing mean-field method results with Brownian dynamics simulation results. The differences between the two methods were a few percent at most. Therefore the mean-field treatment should cause no significant errors, and we employ it for its computational efficiency.

6) Actin polymerization and filament nucleation are treated by rate equations. In order to assess the accuracy of our rate-equation approach, we compare some predictions of this approach with parallel results obtained using a stochastic-growth method that explicitly treats monomer, filament, and branch positions in three dimensions [11,12]. All of the unit processes in this code are treated stochastically. We treat polymerization on a flat $0.5\mu m \times 0.5\mu m$ surface coated with an actin nucleator. We use constant local and bulk concentrations (e.g., $[CP] = [CP_0] = [CP_0']$) in order to focus on potential discrepancies between the rate-equation and stochastic approaches. Branching in the stochastic code is assumed to occur along the sides of filaments, but only within a distance of 10 nm from the surface. The results are obtained as an average over eight runs for each set of parameters. Because k_{br} has a different meaning in the stochastic code compared to the present approach (branching rate per subunit vs. filament tip), we have scaled the k_{br} axis of the stochastic results to line them up with the rate-equation results. As a figure of merit, we use the number of filaments at 30 s as a function of k_{br} and k_{cap}. Figs. S1(a) and S1(b) show that

over a broad range of k_{br} and k_{cap}, the rate-equation and stochastic approaches yield generally similar results. The parameters in the stochastic code were chosen so that almost all of the filaments remain in contact with the surface as the network undergoes retrograde flow. For different parameter sets, where more unfavorably oriented filaments leave the branching region, increasing capping reduces the filament number by a smaller amount. This would tend to strengthen the net positive effect of CP on filament number, that we find below when depletion effects are included.

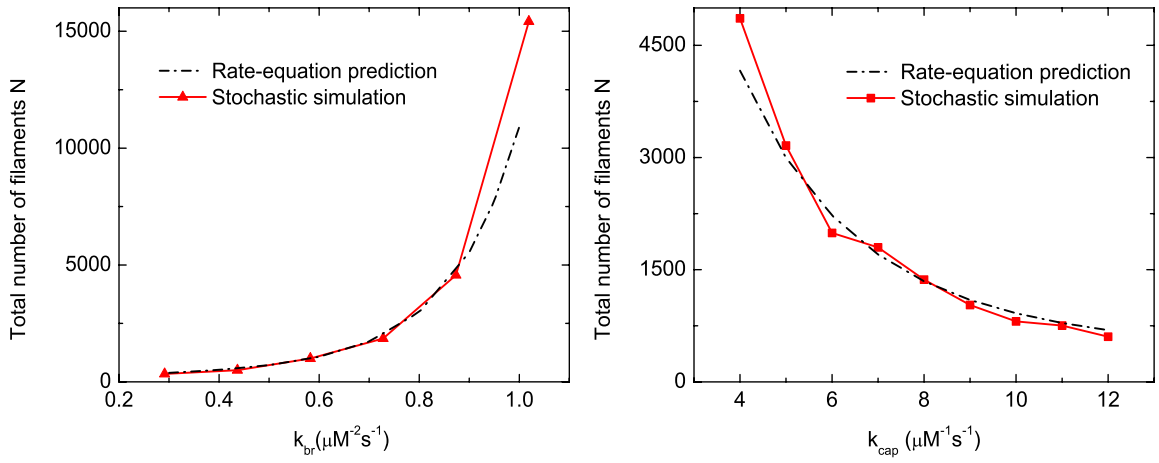

Figure S1: Comparison of present rate-equation model with results from stochastic growth of 3D actin network on patch of surface. $[G_0]$ =0.65 μM, $[CP_0]$ =0.021 μM, k_{sp}=22 $\mu M^{-2}s^{-1}$. For (b): k_{br}=0.65 $\mu M^{-2}s^{-1}$.

C: Derivation of upper limit of CP-generated filament count

Let $C(L)$ be the concentration of CP-nucleated filaments having length L, so that the total concentration of such filaments is $\sum_L C(L)$. We assume that this equals $\Delta[CP]$. If the filaments are nucleated at a constant rate, and grow at a constant rate, then the length distribution will be uniform, so that

$$C(L) = C_0 \equiv \Delta[CP]/(L_{max} - L_{min}), \tag{S1}$$

where L_{max} is the maximum filament length; clearly $L_{max} = 2\langle L\rangle - L_{min}$. Since the diffusion coefficient D_{fil} of a rodlike filament is approximately inversely proportional to its length [13], we take $D_{fil} = D_m/L$. In the limit of a perfectly absorbing bead, beginning with zero attached filaments at time $t = 0$, the number of filaments of length L attached to the bead is given by the Smoluchowski rate theory [14] as $4\pi D_{fil} C(L) r_0(1 + r_0/\sqrt{\pi D_{fil} t})$.

Then the total number of CP-nucleated filaments N_{touch} attached to the bead is

bounded as follows:

$$\frac{dN_{touch}}{dt} \leq \int_{L_{min}}^{L_{max}} 4\pi D_{fil} C(L) r_0 (1 + \frac{r_0}{\sqrt{\pi D_{fil} t}}) dL = 4\pi r_0 C \int_{L_{min}}^{L_{max}} (\frac{D_m}{L} + r_0 \sqrt{\frac{D_m}{\pi L t}}) dL. \tag{S2}$$

Integrating inequality (S2) over time t from 0 to the end time of the experiments at t_f=60s, we obtain

$$N_{touch} \leq N_{touch}^{max} = 4\pi r_0 C_0 [D_m t_f \ln \frac{L_{max}}{L_{min}} + 4 r_0 \sqrt{D_m t_f / \pi} (\sqrt{L_{max}} - \sqrt{L_{min}})] \tag{S3}$$

.

This proves Eq. (11) of the main text.

D: Branching-only model

We showed in the main text that if spontaneous nucleation (SN) is the only source of initiation of actin filaments, the experimental data can well be reproduced. Here we show that a model in which all new filaments are generated by branching beginning with a number of preexisting seed filaments (which could have been generated in solution) also fits the data well. We tried several different seed filament numbers, and found that the differences are negligible (except for at very early times) as long as the number of seed filaments is less than 20% of the final number of filaments. In the results shown in Figs. S2(a) and S2(b) we chose the initial number of seed filaments to be 0.1% of the number of filaments at $t = 60\ s$. It is seen that the experimental results are matched well.

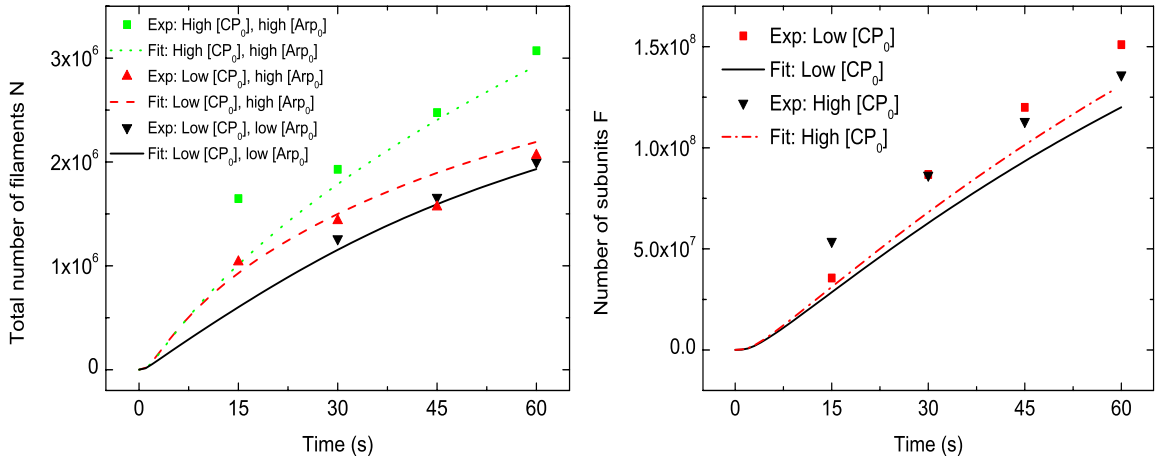

(a) (b)

Figure S2: Branching only model (BN). $[G_0]$ =2.2 μM, k_{br}=0.68 $\mu M^{-2} s^{-1}$, k_{sp}=0, $[Arp_c] = 2\ nM$. Low $[CP_0] =$ 21 nM, high $[CP_0] =$ 52 nM. Low $[Arp_0] =$ 48 nM, high $[Arp_0] =$ 96 nM; $[Arp_0] = 96\ nM$ if unspecified.

E: Analysis of the actin shell thickness and the possible effect of Arp2/3 complex on the network structure

In the experiments of Ref. [4], the actin shell thickness W was found to vary from less than 1 μm, to 2.5 μm, depending on $[Arp_0]$ and $[CP_0]$. A naive estimate of W is that it should be less than the length of single uncapped filament growing out over the whole $60s$ period of the experiment: $W \leq \int_0^{60s} k_{on}[G]\delta dt$. Eq. (1) of the main text shows that the basic laws of diffusion, combined with the polymerization rate obtained in Ref. [4], rigorously imply a strong depletion of the local monomer concentration $[G]$. We find that $\int_0^{60s} k_{on}[G]\delta dt$ is only a few hundred nm, smaller than the observed thicknesses. We believe that the resolution to this apparent discrepancy is that the shell in the experiments is swollen by repulsive interactions between filaments, either steric or electrostatic. These become important at the very high F-actin densities at the surface of the bead. There is substantial evidence for such effects. Ref. [15] found that the mechanical behavior of neutrophils could be described as well by a swelling model as by a model using protrusion forces based entirely on actin polymerization. Furthermore, the simulations of Ref. [16] found that a measured force-velocity relation for branched actin networks could be reproduced by a model which has swelling as an important factor.

To estimate the extent of swelling, we note that the filaments in the experiments have on average about 50 subunits, so we take the aspect ratio (length/diameter) to be 50. Randomly oriented filaments with an aspect ratio of 50 will have a packing fraction of only about 10%, as seen in Fig. 2 of Ref. [17]. The total number of subunits in the network is approximately 1.5 $\times 10^8$ (Fig. 5c of Ref. [4]). Taking an actin filament to have a diameter of 7 nm [18], and using a length increment of 2.7 nm per subunit [19], gives a volume of $1.5 \times 10^8 \times 2.7\ nm \times \pi \times 3.5^2 nm^2/0.1 \simeq 155\ \mu m^3$ for a 10% packing fraction. This corresponds to a thickness of about 1 μm on a bead of radius 3 μm, within the range of observed thicknesses. These findings support the hypothesis of Akin and Mullins [4] that the thickness is influenced by the mechanical properties of the networks rather than just the kinetics of polymerization. As Arp2/3 complex accumulates, it may inhibit actin network remodeling and cause the actin filaments to become denser, reducing the shell thickness.

References

[1] Richard B Dickinson and Daniel L Purich. Diffusion rate limitations in actin-based propulsion of hard and deformable particles. *Biophysical journal*, 91(4):1548–1563, 2006.

[2] Alex Mogilner and Leah Edelstein-Keshet. Regulation of actin dynamics in rapidly moving cells: a quantitative analysis. *Biophysical journal*, 83(3):1237–1258, 2002.

[3] Thomas E Schaus and Gary G Borisy. Performance of a population of independent filaments in lamellipodial protrusion. *Biophysical journal*, 95(3):1393–1411, 2008.

[4] Orkun Akin and R Dyche Mullins. Capping protein increases the rate of actin-based motility by promoting filament nucleation by the Arp2/3 complex. *Cell*, 133(5):841–851, 2008.

[5] Julie Plastino, Ioannis Lelidis, Jacques Prost, and Cécile Sykes. The effect of diffusion, depolymerization and nucleation promoting factors on actin gel growth. *European Biophysics Journal*, 33(4):310–320, 2004.

[6] F Lanni and BR Ware. Detection and characterization of actin monomers, oligomers, and filaments in solution by measurement of fluorescence photobleaching recovery. *Biophysical journal*, 46(1):97–110, 1984.

[7] Howard C. Berg. *Random Walks in Biology*. Princeton University Press, 1993.

[8] David Sept and J Andrew McCammon. Thermodynamics and kinetics of actin filament nucleation. *Biophysical journal*, 81(2):667–674, 2001.

[9] Jonathan Zalevsky, Leah Lempert, Heather Kranitz, and R Dyche Mullins. Different WASP family proteins stimulate different Arp2/3 complex-dependent actin-nucleating activities. *Current Biology*, 11(24):1903–1913, 2001.

[10] Scott H Northrup. Diffusion-controlled ligand binding to multiple competing cell-bound receptors. *The Journal of Physical Chemistry*, 92(20):5847–5850, 1988.

[11] Anders E Carlsson. Growth of branched actin networks against obstacles. *Biophysical journal*, 81(4):1907–1923, 2001.

[12] Anders E Carlsson. Dendritic actin filament nucleation causes traveling waves and patches. *Physical review letters*, 104(22):228102, 2010.

[13] M. Doi and S. F. Edwards. *The Theory of Polymer Dynamics*. Clarendon Press, Oxford, 1998.

[14] Sidney Redner. *A guide to first-passage processes*. Cambridge University Press, 2001.

[15] Marc Herant, William A Marganski, and Micah Dembo. The mechanics of neutrophils: synthetic modeling of three experiments. *Biophysical journal*, 84(5):3389–3413, 2003.

[16] Christian H Schreiber, Murray Stewart, and Thomas Duke. Simulation of cell motility that reproduces the force–velocity relationship. *Proceedings of the National Academy of Sciences*, 107(20):9141–9146, 2010.

[17] SR Williams and AP Philipse. Random packings of spheres and spherocylinders simulated by mechanical contraction. *Physical Review E*, 67(5):051301, 2003.

[18] G.M. Cooper and R.E. Hausman. *The Cell: A Molecular Approach*. ASM Press, 2007.

[19] Roberto Dominguez and Kenneth C Holmes. Actin structure and function. *Annual review of biophysics*, 40:169, 2011.